Molecular Therapy
Oncology
Original Article

IL-12-mediated toxicity from localized oncolytic virotherapy can be reduced using systemic TNF blockade

Miriam Valenzuela-Cardenas,[1] Carrie Fisher,[2] Mee Y. Bartee,[1] and Eric Bartee[1]

[1]Department of Internal Medicine, University of New Mexico Health Sciences Center, Albuquerque, NM, USA; [2]Department of Microbiology and Immunology, Medical University of South Carolina, Charleston, SC, USA

Cytokine therapy represents an attractive option to improve the outcomes of cancer patients. However, the systemic delivery of these agents often leads to severe immune-related toxicities, which can prevent their efficient clinical use. One approach to address this issue is the use of recombinant oncolytic viruses to deliver various cytokines directly to the tumor. This improves the biodistribution of the secreted cytokine-transgenes, both augmenting antitumor immune responses and decreasing systemic toxicities. We have shown recently that a doubly recombinant oncolytic myxoma virus that secretes a soluble version of PD1 as well as an interleukin-12 (IL-12) fusion protein (vPD1/IL-12) can cause potent regression of disseminated cancers. Here we show that, despite the predominant localization of both transgenes within the infected tumor, treatment with vPD1/IL-12 still results in systemic, IL-12-mediated toxicities. Interestingly, these toxicities are independent of interferon-γ and instead appear to be mediated by the interaction of tumor necrosis factor α with tumor necrosis factor receptor 2 on hematopoietic cells. Critically, this unique mechanism allows for vPD1/IL-12-mediated toxicities to be alleviated through the use of US Food and Drug Administration (FDA)-approved tumor necrosis factor (TNF) blockers such as etanercept.

INTRODUCTION

Oncolytic virotherapy (OV) uses replication-competent viruses to treat a variety of cancers.[1] One of the main advantages of OV is that the tumor-tropic replication of the viral agents creates the opportunity to deliver potentially toxic proteins directly into the tumor microenvironment (TME).[2–4] This can increase the local concentration of these agents, thus potentially improving therapeutic efficacy, while also alleviating the development of systemic toxicities.

We have recently described a novel, doubly recombinant oncolytic myxoma virus (MYXV) that encodes a soluble version of programmed cell death 1 (PD1) as well as an interleukin-12 (IL-12) fusion protein (termed vPD1/IL-12) and shown that this virus is highly effective at regressing both injected and non-injected tumors from a variety of different cancer types.[5] However, while the MYXV backbone has been proven to be non-toxic in numerous preclinical models, both PD1/PD-L1-blockade and IL-12-based therapies are associated with the development of potentially severe immune related toxicities (IRTs). For example, PD-L1 blockade has been shown to cause itching and rash, gastrointestinal symptoms such as diarrhea and colitis, thyroid dysfunction commonly manifesting as hypothyroidism and hyperthyroidism, pituitary inflammation, and musculoskeletal toxicities, including mild joint and muscle pain.[6–8] Similarly, systemic IL-12 treatment causes numerous minor side effects, such as fatigue, vomiting, diarrhea, and headaches, which resemble flu-like symptoms,[9,10] as well as more severe complications, including hematopoietic issues such as leukopenia, anemia, neutropenia, and decreased platelets and clotting ability, known as thrombocytopenia,[11–13] and hepatocellular damage, commonly presenting as increased liver enzymes, like alanine aminotransferase (ALT) and aspartate transaminase (AST).[14] Critically, while many of the IRTs associated with PD1 blockade can be managed effectively, the same cannot be said for IL-12 therapy, whose systemic use is largely precluded by the extensive and severe nature of the toxicities observed following treatment. Mechanistically, the toxicities induced by both PD1 blockade and IL-12 are often linked to the secondary secretion of cytotoxic effectors such as interferon-γ (IFNγ) and tumor necrosis factor alpha (TNF-α) which can also play essential roles in the therapeutic efficacy of these treatments.[10,15,16] The clinical translation of any therapy based on these agents therefore requires a complete understanding of the molecular mechanisms involved in both therapeutic efficacy as well as associated toxicities.

In the current work, we examined the toxicity profiles induced by vPD1/IL-12 treatment in a variety of murine tumor models. Our results show that, despite the fact that most of the virally expressed PD1 and IL-12 are retained within the treated tumor, localized treatment with this virus still induces IL-12-mediated pathologies, including hematopoietic defects and liver toxicities. Interestingly, these toxicities are independent of IFNγ and instead appear to be mediated by the interaction of TNF with TNF receptor 2 (TNFR2), which allows

Received 23 May 2024; accepted 23 August 2024;
https://doi.org/10.1016/j.omton.2024.200866.

Correspondence: Eric Bartee, University of New Mexico Cancer Research Facility, 1 University of New Mexico, MSC07 4025, Albuquerque, NM 87131, USA.
E-mail: ebartee@salud.unm.edu

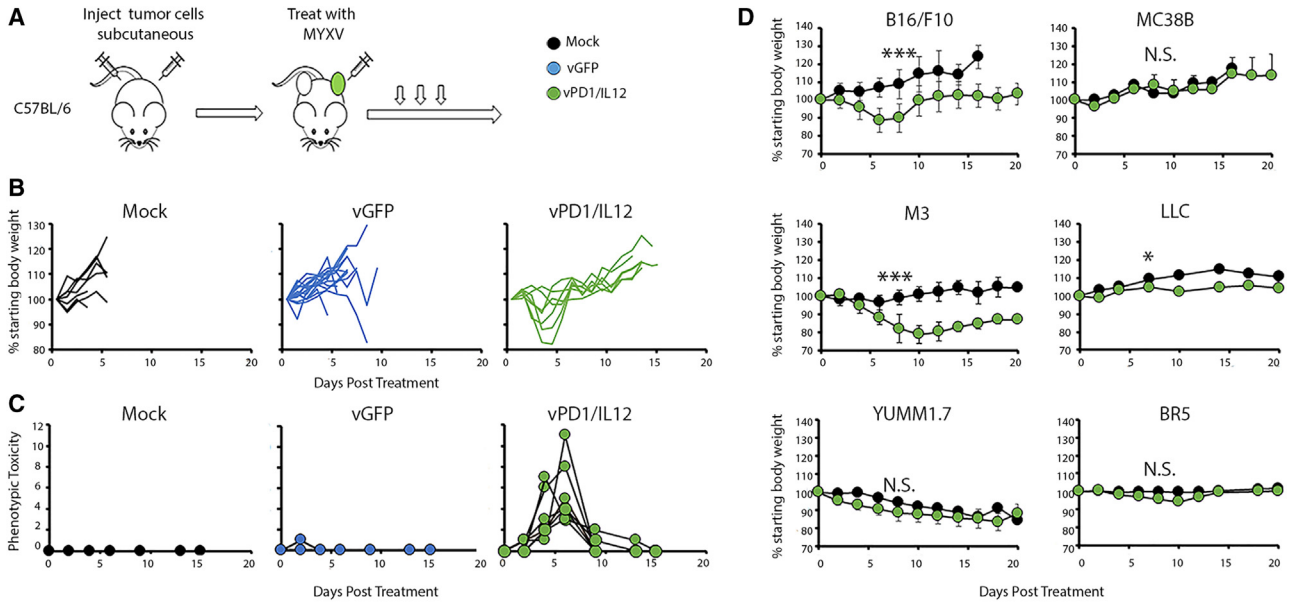

Figure 1. Localized treatment with vPD1/IL-12 results in observable signs of systemic toxicity

(A) Schematic of the experimental design. Mice were injected s.c. on the left and right flanks with tumor cells. After allowing for tumor establishment, mice were either mock treated or treated with three injections of the virus IT. Weights and body wellness score criteria were assayed for the duration of the study. (B) Weight measurements for individual mice treated as indicated. Data are presented as a percent change from initial weight (n = 7/cohort). (C) Phenotypic toxicity scores for individual mice graphed as an overall score at different time points, peaking at day 8 in vPD1/IL-12-treated cohorts (n = 7/cohort). (D) Weight for both saline- and vPD1/IL-12-treated mice bearing the indicated type of tumor. Data represent the average weight for all animals in the indicated cohort, presented as the percent change from starting weight (n = 5–20 mice/cohort). Significance was determined using Student's t test at day 8 post treatment (*$p < 0.05$, ***$p < 0.001$; N.S., not significant).

them to be alleviated using US Food and Drug Administration (FDA)-approved TNF blockers.

RESULTS

Localized treatment with vPD1/IL-12 results in systemic toxicity

To determine whether treatment with vPD1/IL-12 induced any systemic toxicities, we treated mice bearing contralateral, subcutaneous (s.c.) B16/F10 melanomas with three intratumoral (IT) doses of either saline or 1×10^7 focus-forming units (FFUs) of either vPD1/IL-12 or a non-armed, control MYXV expressing GFP (vGFP) (Figure 1A). Mice were then monitored for weight loss or scored for "phenotypic toxicity" based on various observable parameters, including changes in body position, dehydration, decreased body temperature, decreased activity and strength, loss of grooming, blepharospasm, and changes in consistency of stool (Table S1). The results indicated that groups treated with vPD1/IL-12 displayed transient weight loss of up to 15% of their body weight beginning around 3 days post treatment and lasting until 6–8 days post treatment (Figure 1B). This weight loss corresponded with a similarly timed increase in "phenotypic toxicity" score (Figure 1C). Neither weight loss nor changes in body condition were observed in either saline- or vGFP-treated mice. Interestingly, similar studies in vPD1/IL-12-treated mice bearing other types of tumors suggested that the development of toxicities following viral treatment varied between tumor models. Similar to mice bearing B16/F10 melanomas, mice bearing M3 (melanoma) and Lewis lung carcinoma (LLC; lung cancer) tumors displayed statistically significant weight loss following treatment with vPD1/IL-12. Despite the transient display of toxicity, these issues did not appear to be dose limiting, and all mice treated with vPD1/IL-12 eventually recovered. In contrast, mice bearing MC38 (colon cancer), BR5 (ovarian cancer), or YUMM1.7 (melanoma) tumors maintained their weight (Figure 1D).

To further quantify the molecular events that might be mediating our observed "phenotypic toxicity," we also analyzed B16/F10 melanoma-bearing mice treated with saline or vPD1/IL-12 for changes in their hematologic compartment or serum blood chemistry 8 days after initial viral treatment. The results indicated that mice treated with vPD1/IL-12 displayed a wide range of both hematological and chemical changes compared to mice treated with saline (Figures 2A–2D). Within the hematological compartment, these changes included a significant decrease in red blood cell concentration, which acutely affected hematocrit, hemoglobin, and other parameters associated with red blood cell integrity, as well as an increase in neutrophils and a decrease in lymphocytes (Figure 2A). Similarly, changes in various blood chemistry parameters were observed, such as decreased glucose (GLU), serum albumin (ALB), and total protein (TP) and increases in a variety of liver enzymes indicative of hepatocellular damage, including ALT, alkaline phosphatase (ALP), and AST (Figure 2B). Other assayed criteria that did not differ between treatment groups are shown in (Figure S1). Due to high mouse-to-mouse variation in individual parameters, to help quantify these toxicities, we developed both "hematopoietic" and "blood chemistry" toxicity scoring systems that summarized all

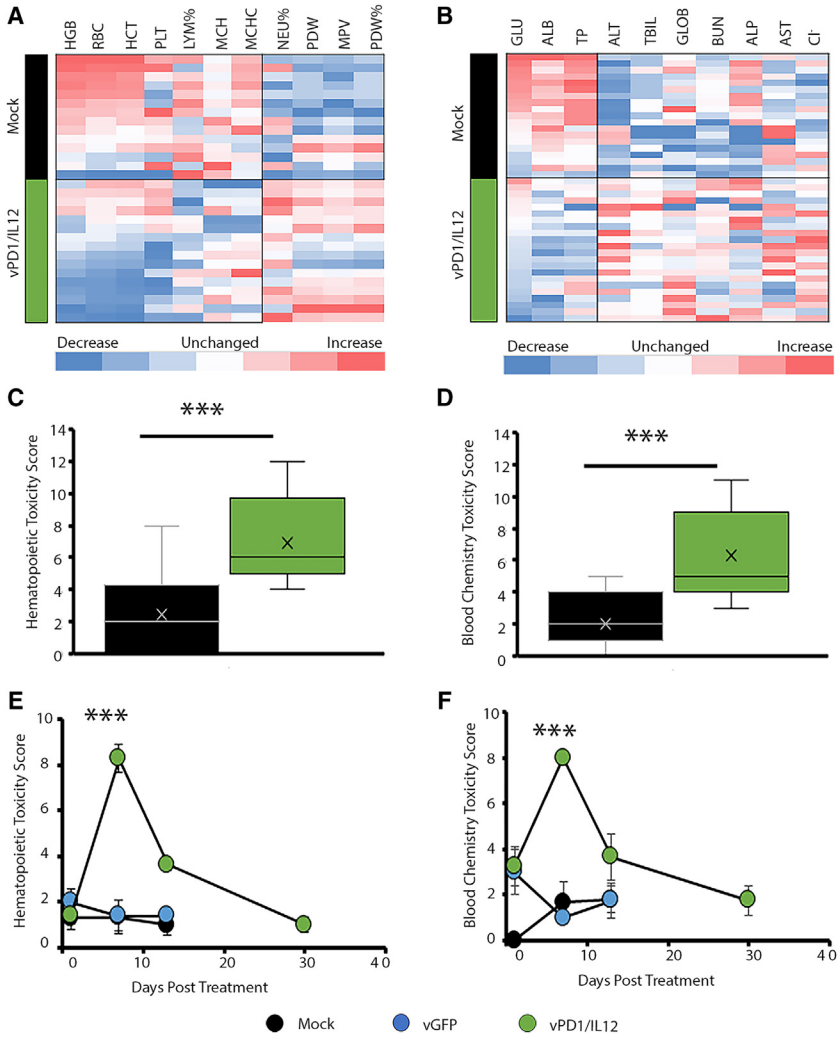

Figure 2. Localized treatment with vPD1/IL-12 results in both chemical and hematopoietic changes

(A and B) Heatmap analyses showing changes to the indicated hematological (A) or chemical (B) parameters. Each row indicates an individual mouse (n = 14–22). The graphical display corresponding to upregulation and downregulation is calculated individually for each parameter due to the high variability and the lack of consistency in the magnitude of changes between mock and treated cohorts. (C) Quantification of hematopoietic toxicity score. (D) Quantification of blood chemistry toxicity score. (E and F) Time-course comparison of hematopoietic and blood chemistry toxicity score between cohorts (n = 2–7/cohort/time point). Significance was determined by comparing vPD1/IL-12-treated samples to vGFP-treated samples at day 6 using Student's t test (***$p < 0.001$).

of the analyzed parameters into a single toxicity score (Tables S2 and S3). Overall, these scoring systems demonstrated that vPD1/IL-12 induces significant hematological and chemical toxicities in treated mice (Figures 2C and 2D). Finally, to determine whether the molecular toxicities identified in our screen displayed resolution kinetics similar to the "phenotypic" toxicities we had documented previously, mice bearing B16/F10 melanomas were treated with three IT doses of either saline or 1×10^7 FFUs of vGFP or vPD1/IL-12, and then tissues were harvested at various times post treatment for molecular and chemical analysis. In accordance to the gross physiological changes and weight loss observed following vPD1/IL-12 treatment, the results indicated that both the hematological and chemical toxicity scores induced by viral treatment peaked at day 8 post treatment and then quickly decreased, returning back to baseline by day 30 (Figures 2E and 2F). Altogether, these data suggest that localized treatment with vPD1/IL-12 induces a systemic form of toxicity characterized by phenotypic, hematopoietic, and chemical changes that begin 3–8 days post treatment and subsequently resolve.

vPD1/IL-12-mediated toxicity results from the leaky biodistribution of its IL-12 transgene

One of the conceptual advantages of using an oncolytic virus to deliver otherwise toxic transgenes is that the expression of these payloads is generally restricted to the tumor.[17–20] To confirm whether this was true for vPD1/IL-12, we assayed the previously acquired samples (from Figure 2D) for the presence of infectious viral progeny, soluble PD1, and IL-12. Consistent with previous literature, high titers of infectious MYXV could be isolated from directly injected tumor lesions (Figure 3A). In contrast, infectious virus could not be consistently isolated from either the non-injected tumors or from any other organ assayed, including the kidneys, stomach, lungs, large or small intestine, heart, liver, bone marrow, or blood (Figures 3A and S2A). While the levels of both the secreted PD1 and IL-12 transgenes were highest in the directly injected tumor, a significant increase in the levels of both products could also be detected in the blood of treated mice 6 days post viral infection (Figures 3B and S2B). Based on these data, we hypothesized that vPD1/IL-12's toxicity might result from the leaky biodistribution of its transgenes. To test this hypothesis, either wild-type or IL-12 receptor β1 subunit-deficient (*IL-12RB1*$^{-/-}$) mice bearing B16/F10 melanomas were treated with three IT doses of either saline or 1×10^7 FFUs of vPD1/IL-12 and then monitored for weight loss. The results indicated that, while wild-type (WT) mice displayed the anticipated weight loss following viral treatment, *IL-12RB1*$^{-/-}$ mice maintained their weight following vPD1/IL-12 treatment (Figures 3C and S3A). Since most of IL-12's previously reported toxicities are the result of systemic immune activation, we further asked whether loss of various immune components would alleviate these issues following vPD1/IL-12 therapy. To test this, either WT or completely immune-deficient non-obese diabetic/severe combined immunodeficiency/*IL-2Rγ*$^{-/-}$ (NSG) mice bearing B16/F10 melanomas were treated as above and then monitored for weight loss. Consistent with IL-12 inducing

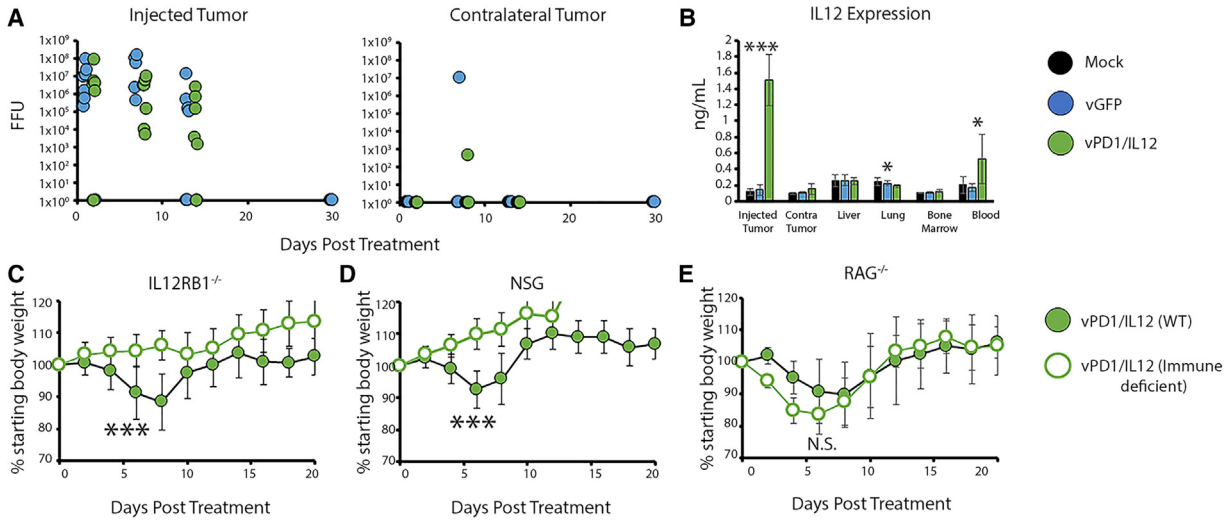

Figure 3. vPD1/IL-12-mediated toxicity results from the leaky biodistribution of its IL-12 transgene

(A) Number of infectious viral progeny recovered from both injected and contralateral tumors at the indicated time points (n = 7–12/cohort/time point). Each circle represents data from a single animal. (B) Abundance of IL-12 in the indicated tissues (n = 7–8/cohort). (C–E) Weight for either C57Bl/6 mice or mice of the indicated knockout strain bearing B16/F10 tumors treated with PD1/IL-12. Data represent the average weight for all animals in the indicated cohort, presented as the percent change from starting weight (n = 5–10 mice/cohort). Significance was determined at day 6 using Student's t test (***$p < 0.001$).

systemic IRTs, WT mice lost weight following treatment, while NSG mice maintained their weight (Figures 3D and S3B). In contrast, T and B cell-deficient, recombination-activating gene ($RAG^{-/-}$) mice actually displayed a trend toward increased weight loss following viral treatment (Figures 3E and S3C). These data suggest that vPD1/IL-12's toxicities are the result of its IL-12 transgene inducing IRTs through activation of a non-T or B immune cell.

Loss of TNF reduces vPD1/IL-12-mediated toxicity

While IL-12 has a well-established toxicity profile, much of this toxicity is mediated indirectly through the induction of secondary inflammatory mediators such as IFNγ.[10,15,16] Consistent with this, bulk transcriptomic analysis of tumor tissue from mice bearing B16/F10 melanomas treated with three IT doses of saline, 1×10^7 FFUs, vGFP, or vPD1/IL-12 showed a significant upregulation of a variety of inflammatory effector molecules, including TRAIL, IFNγ, IL-6, and TNF following vPD1/IL-12 treatment (Figure 4A). These results were confirmed using ELISA-based biodistribution analysis, which demonstrated an upregulation of IFNγ, IL-6, and TNF (Figure 4B). Interestingly, this analysis also demonstrated that, while expression of IL-6 was largely confined to the tumor tissue, increased levels of both IFNγ and TNF were found throughout a variety of murine tissues (Figure 4B). Surprisingly, no reads for either IFNα or IFNβ were identified. Based on these data, we further examined the potential role of both IFNγ and TNF in vPD1/IL-12-induced toxicities. Interestingly, while a variety of previous work has implicated IFNγ as a major mediator of IL-12's toxicities, mice lacking IFNγ or the IFNγ receptor still displayed significant weight loss following vPD1/IL-12 therapy (Figure S4). In contrast, vPD1/IL-12-treated mice lacking TNF displayed significantly less weight loss than comparable WT animals (Figure 4C). Additionally, these mice also displayed lower hematopoietic and chemical toxicity scores, with the hematopoietic score being statistically indistinguishable from that of non-treated animals (Figure 4D). While neither score quite reached statistical significance alone, combining the scores to generate an overall toxicity score showed that, while TNF-deficient mice still displayed some signs of molecular toxicity, this toxicity was significantly reduced compared to that seen in WT mice (Figure 4E). Taken together, these data suggest that elimination of TNF reduces vPD1/IL-12's toxicity profile, particularly within the hematopoietic compartment.

TNF mediates vPD1/IL-12 toxicity through TNFR2 expressed on hematopoietic cells

TNF mediates its biological effects through two different receptors, which are differentially expressed on various cell types. TNF receptor 1 (TNFR1) is found on virtually all cells, while TNF receptor 2 (TNFR2) is found predominately on specific subsets of immune cells as well as endothelial and neuronal cells.[21,22] To understand how exactly TNF was mediating the physical changes we observed following viral treatment, we treated B16/F10 melanoma-bearing mice deficient in either TNFR1 or TNFR2 with vPD1/IL-12 and then monitored their weight loss. The results indicated that mice lacking TNFR1 displayed weight loss similar to that seen in WT controls. In contrast, mice lacking TNFR2 displayed significantly reduced levels of weight loss following vPD1/IL-12 treatment (Figure 5A). Since TNFR2 is expressed on both hematopoietic and non-hematopoietic cells, we next asked which of these cell types was responding to TNF during our therapy. To address this question, we generated as series of bone marrow chimeric mice in which either WT bone marrow was transplanted into $TNFR2^{-/-}$ mice or

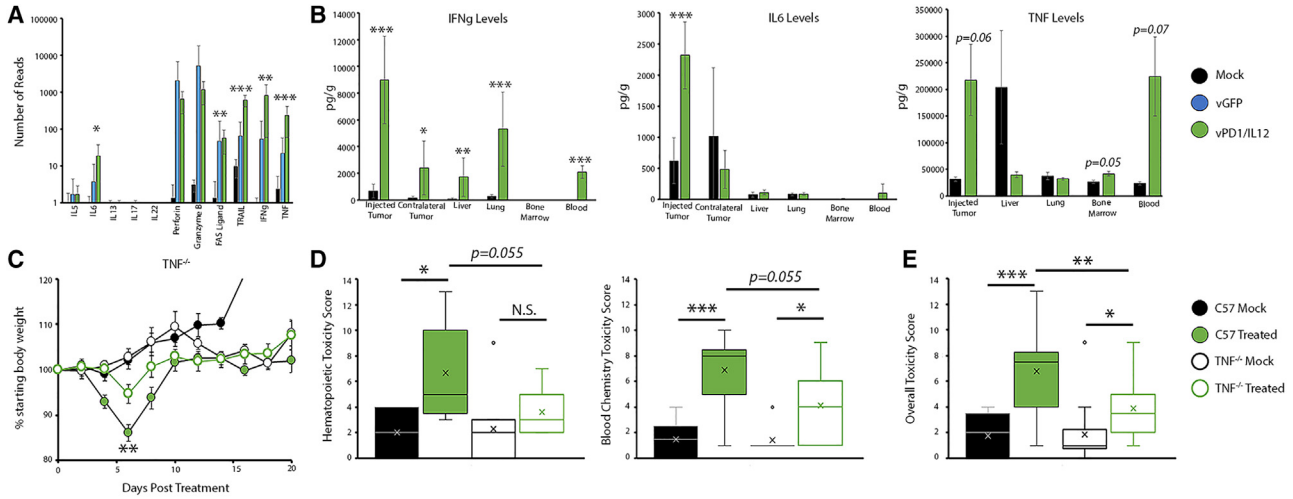

Figure 4. vPD1/IL-12-mediated toxicity requires TNF

Tumors that were either mock treated or treated with vGFP or vPD1/IL-12 were harvested, and RNA was extracted for bulk RNA sequencing. (A) Analysis of the number of total reads for the indicated cytokines. (B) ELISA and cytometric bead array quantification of the indicated cytokines in various tumor and tissue samples following treatment. (C) Weight for B16/F10 melanoma-bearing C57Bl/6 or *TNF*$^{-/-}$ mice treated as indicated. Data represent the average weight for all animals in the indicated cohort, presented as the percent change from starting weight (n = 13–20 mice/tumor model in each cohort). (D) Quantification of the indicated toxicity scores between mock- and vPD1/IL-12-treated cohorts in WT mice compared to mock- and vPD1/IL-12-treated cohorts in mice lacking TNF. (E) Overall toxicity score generated by combining the hematopoietic and blood chemistry toxicity scores. Significance for all charts was determined using Student's t test (*$p < 0.05$, **$p < 0.01$, ***$p < 0.001$).

TNFR2$^{-/-}$ bone-marrow was transplanted into WT mice. Six weeks after bone marrow transplantation, the chimerism of each mouse was confirmed (Figure S5), and then B16/F10 melanomas were established on each animal. Tumors were subsequently treated with three IT doses of either saline or 1×10^7 FFUs of vPD1/IL-12, and animals were monitored for weight loss. The results indicated that chimeric mice lacking TNFR2 on non-hematopoietic cells but expressing TNFR2 within the hematopoietic compartment displayed levels of weight loss similar to WT mice (Figure 5B). In contrast, mice lacking TNFR2 specifically within the hematopoietic compartment displayed reduced weight loss following vPD1/IL-12 treatment (Figure 5C). All mock-treated mice exhibited no weight loss (Figure S6). When we analyzed for the molecular components of toxicity, the molecular profiles suggested that lack of TNFR2 led to a significant improvement in the hematologic toxicity parameters but no change in the blood chemistry toxicity score (Figure 5D). These results suggest that weight loss and physical representations of toxicity are driven primarily as a result of the changes in the hematologic compartment and are less impacted by changes in the blood chemistry criteria. Overall, these results confirm that TNF induced by vPD1/IL-12 therapy mediates toxicity in this model by interacting with TNFR2 expressed on hematopoietic cells.

Treatment with clinically applicable TNF blockade can alleviate vPD1/IL-12-associated toxicity

Our previous results demonstrated that localized vPD1/IL12 therapy is associated with a variety of detrimental effects caused by its IL-12 transgene inducing systemic expression of TNF. Importantly, due to IL-12's checkered past, this could severely limit the therapeutic application of this virus. However, our mechanistic studies suggested that these toxicities could be largely alleviated by blocking the interaction of TNF with TNFR2. To determine whether this could be applied in a therapeutic setting, we tested whether the systemic injection of TNF-blocking agents could reduce the toxicities induced by vPD1/IL-12 therapy (Figure 6A). B16/F10 melanoma-bearing animals were treated with three IT doses of either saline or 1×10^7 FFUs of vPD1/IL-12. Immediately after viral treatment, vPD1/IL12-treated animals were further segregated into two cohorts and injected with either an anti-TNF blocking antibody[23] or an isotype control and then monitored for weight loss. Consistent with our working model, animals treated with anti-TNF blocking antibodies displayed less overall weight loss as well as a faster recovery following viral treatment (Figure 6B). Critically, similar results were obtained using the FDA-approved TNF inhibitor etanercept in virally treated mice bearing either B16/F10 and M3 melanomas (Figures 6C and 6D). Taken together, these data suggest that the toxicities associated with vPD1/IL-12 therapy can be alleviated using already clinically accessible TNF inhibitors.

DISCUSSION

IL-12 has shown tremendous preclinical success in multiple models of malignancy. The use of this immunotherapy, however, has been largely precluded by the severe IRTs associated with systemic treatment.[10–16] Our lab has previously generated a doubly recombinant oncolytic virus that expresses both soluble PD1 and IL-12 and shown that this virus is highly efficacious in a variety of tumor models.[5] In the current work, however, we show that treatment with this virus also causes a series of systemic toxicities. These toxicities manifest

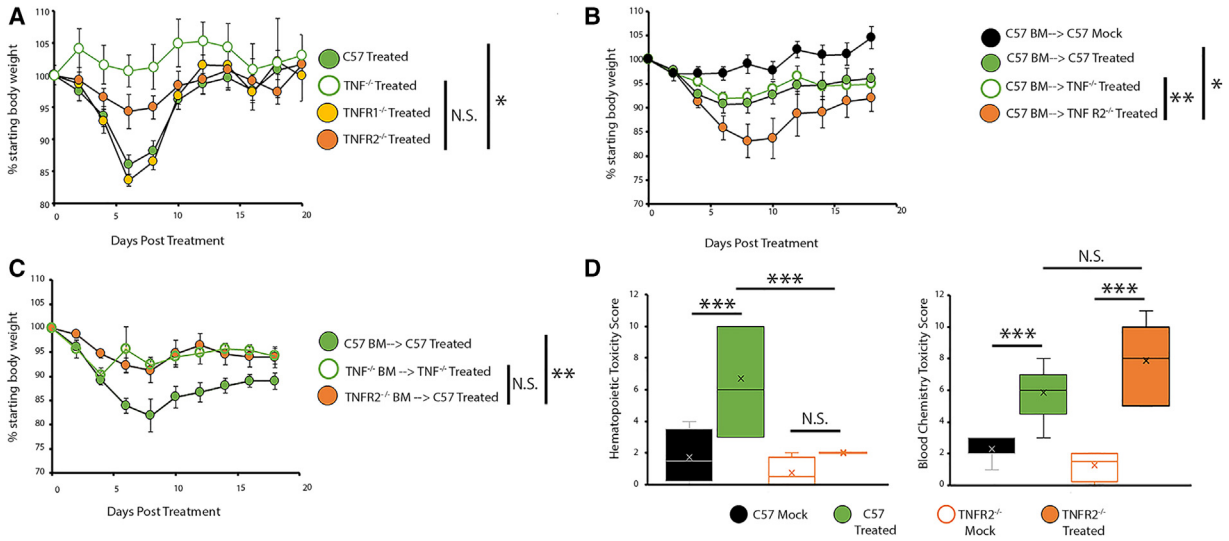

Figure 5. TNF mediates vPD1/IL-12 toxicity through TNFR2 expressed on hematopoietic cells

Weight for either C57Bl/6 mice or mice of the indicated strain bearing B16/F10 melanomas treated with PD1/IL-12. Data represent the average weight for all animals in the indicated cohort, presented as the percent change from starting weight (n = 3–5 mice/tumor model in each cohort). (B–D) The indicated chimeric animals were generated using bone marrow transplants. (B and C) Weight for the indicated chimeras bearing B16/F10 melanomas treated with PD1/IL-12. Data represent the average weight for all animals in the indicated cohort, presented as the percent change from starting weight (n = 3–6 mice/tumor model in each cohort). (D) Hematopoietic and blood chemistry toxicity scores for the indicated cohorts 6 days post viral treatment (n = 4–7 mice/cohort). Significance was determined for the indicated comparisons at day 6 using Student's t test (*$p < 0.05$, **$p < 0.01$, ***$p < 0.001$).

as weight loss, physical ailments, and molecular changes within the hematopoietic compartment and serum chemistry and are derived primarily from the production of IL-12. Interestingly, the individual parameters typically used to quantify toxicity displayed extremely high levels of variation in our experiments, both between individual mice within a single experiment and between replicate experiments. For instance, in one experiment, ALT would be highly elevated and AST would be unchanged, while in a second experiment, AST would be elevated and ALT unchanged. Both of these parameters indicate liver damage, but the high variation made statistical analysis of individual parameters difficult. To quantify these toxicities, we therefore chose to create a method to look at the toxicity profile as a whole without having to focus on single parameters. This was accomplished through the creation of our toxicity scores, which reduce the highly complex and variable data into a single number. While these scoring systems do not have any concrete clinical relevance to humans (i.e., they are not derived from human data), it is important to note that the toxicities we observed are highly similar to those seen in human patients following treatment with IL-12.[9–13] We therefore feel that this approach is an appropriate method to quantify the complex IRTs seen in our studies.

Interestingly, these toxicities were only observed in a subset of tumor models, including B16/F10 and M3 melanomas, as well as LLC lung cancers. In contrast, in YUMM1.7 melanomas, MC38B colon cancer tumors, or BR5 ovarian tumors, viral treatment did not appear to induce any observable signs of toxicity (Figure 1D). The reasons for this distinction are not currently known. It is attractive to hypothesize that toxic models result from higher levels of intratumoral viral replication; however, this does not appear to be the case, since MC38B colon cancer tumors support a high viral load (Figure S7), but mice bearing these tumors do not display overt signs of toxicity (Figure 1D). This suggests a more distinct molecular explanation, such as release of TNF from the cell surface by the protease TACE/Adam, might play a role. Additional experiments are therefore needed to further elucidate the pathways leading to toxic vs. non-toxic tumors.

There have been previous efforts to decrease IL-12-mediated toxicities induced in various settings.[11,24,25] Priming with a low dose of IL-12 before administering a full dose has had some success at decreasing the intensity of side effects; however, this approach has not been perfect,[14,26–28] and is likely not feasible in the context of OV. More in line with our current approach are a variety of attempts to adjust the delivery method of IL-12, including the use of targeted delivery.[29–32] OV provides the perfect platform for this localized delivery; however, this approach also runs the risk of severely decreasing IL-12-mediated efficacy in metastatic lesions.[29,33–36] It is therefore important to note that vPD1/IL-12 has shown efficacy again both injected and non-injected lesions in various tumor models.[5]

Interestingly, while vPD1/IL12's transgenes are produced exclusively from infected tumor cells, both transgenes can also be found in the blood. This raises the strong possibility that the systemic toxicities observed in our treatments result from a "leaky" biodistribution profile in which IL-12 produced in the tumor eventually exits this tissue, resulting in immune activation and systemic effects like that of IL-12

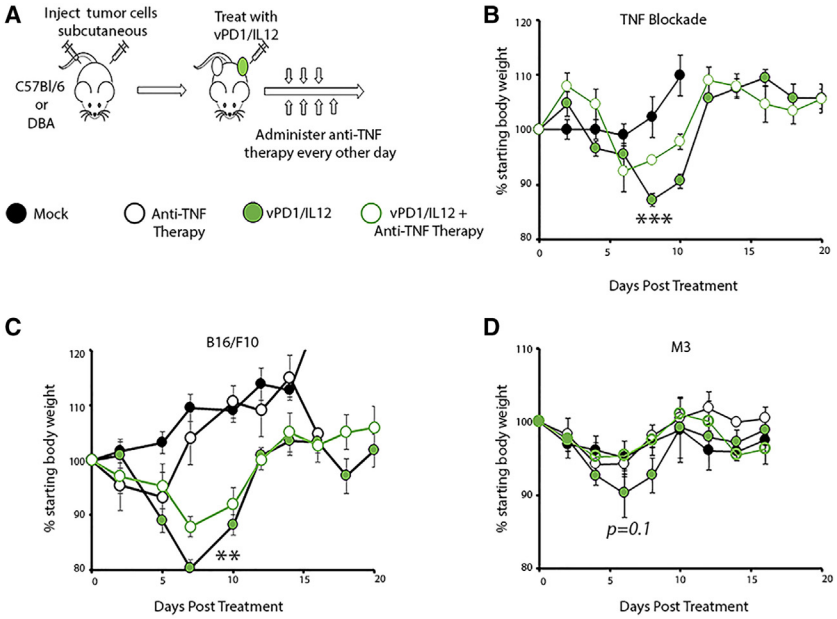

Figure 6. Treatment with clinically applicable TNF blockade can alleviate vPD1/IL-12-associated toxicity

(A) Schematic of the experimental design. (B) Weight for B16/F10 melanoma-bearing animals treated with either saline or vPD1/IL-12 ± anti-TNF blocking antibody. Data represent the average weight for all animals in the indicated cohort, presented as the percent change from starting weight (n = 5/cohort). (C and D) Weight for either B16/F10 (C) or M3 (D) melanoma-bearing animals treated with either saline or vPD1/IL-12 ± etanercept. Data represent the average weight for all animals in the indicated cohort, presented as the percent change from starting weight (n = 3–6 mice/each cohort). Significance was determined for the indicated comparisons at day 7 or 8, respectively, using Student's t test (**$p < 0.01$, ***$p < 0.001$).

monotherapy. If this is the case, then it is possible that the toxicities from vPD1/IL-12 could be alleviated by altering the IL-12 transgene in such a way as to improve its tumor tropism. A variety of these methods have been proposed previously, including only encoding a single-chain IL-12 in order to enhance bioactivity,[37] anchoring IL-12 to tumor cell surface through fusion of the transmembrane domain,[38] or deleting the N-terminal signal peptide to prevent secretion.[39] Our results suggest that incorporation of these alterations into our existing oncolytic vector might be worthwhile.

Most of the existing literature suggests that the toxicities associated with IL-12 monotherapy are the result of systemic immune activations leading to the production of pro-inflammatory cytokines, most notably IFNγ.[15] Specifically, IL-12 has been known to hyperactivate both macrophages and natural killer cells in the liver, leading to hepatomegaly, lymphocyte infiltration, hepatocyte necrosis, and overall liver damage.[40,41] Similarly, IL-12-induced IFNγ has also been tied to decreased leukocyte counts and overall myelo-suppression.[42] Since this toxicity profile closely mirrors that observed in our experiments, it is interesting to note that the toxicities observed in our studies appear to be completely independent of IFNγ, since they were not observed in mice lacking IFNγ or IFNγR1 (Figure S4). Unfortunately, the reasons for this difference are not clear. Our vPD1/IL-12 virus encodes its IL-12 transgene as a p40-p35 fusion protein, which could induce distinct biological toxicities compared to more traditional heterodimers. Alternatively, the fact that that majority of our IL-12 is produced within the TME might also be playing a role. Regardless, it is important to note that, since our toxicities appear to be mediated through a mechanism distinct from most previous IL-12 studies, some of our mechanistic findings might be unique to this system.

When searching for other signaling molecules that could be produced by IL-12 activation, we found that production of a variety of other pro-inflammatory cytokines was significantly higher following vPD1/IL-12 therapy.[15] In particular, reads from both IL-6 and TNF were increased following treatment (Figure 4A). This is consistent with previous clinical studies in which IL-6 and TNF were both observed following IL-12 monotherapy. In our current work, we chose to focus on the role of TNF. However, IL-6 has also been implicated in promoting toxicity in the context of immune checkpoint blockade, and IL-6-blockade can decrease toxicity in the form of enterocolitis and improve antitumor immunity by promoting T_h1 T cell activity.[28,43] Despite IL-6 being a candidate for eliciting toxicity following vPD1/IL-12 therapy, we found that IL-6 localization was restricted primarily to the injected tumor, with very little observed in the blood (Figure 4B). Therefore, while we cannot rule out a role for IL-6 in vPD1/IL12's toxicity, we feel that it is unlikely to be a major molecular driver.

One of the major findings of our paper is that the toxicities induced by our viral treatments are dependent on the expression of TNF. This is consistent with some previous work that has implicated TNF in IL-12-mediated toxicities.[44] Interestingly, in contrast to the systemic use of IL-12 as an anti-cancer therapy, most of the work implicating TNF as a mediator of IL-12 toxicity has come in the context of viral infections, where it has been reported to trigger weight loss and decreased body wellness.[44] These data raise the possibility that the presence of our oncolytic virus itself might be playing a role in the differential impact of TNF and IFNγ in our results. Molecularly, we show that lack of TNFR2 is protective against vPD1/IL-12's toxicities. However, it is noted that the lack of TNFR2 does not eliminate all the negative side effects. Molecular analysis showed that lack of TNFR2 significantly improved hematopoietic toxicities, characterized by leukopenia-, anemia-, thrombocytopenia-, and red blood cell integrity-associated parameters; however, it did not have any effect on the blood chemistry-associated toxicities, including increased liver enzymes suggestive of hepatocellular damage (Figure 5). These data

suggest that treatment-associated toxicity could be taking place through two different pathways. The first affects weight loss and hematopoietic parameters, which can be improved by blocking TNF interaction with TNFR2. The second is responsible for the liver toxicities and is independent of TNFR2. Interestingly, although the liver toxicity does not appear to be mediated by TNFR2 signaling, it was reduced fully in TNF-deficient animals, suggesting that more research is necessary to mechanistically understand the differences that dictate the molecular toxicities taking place.

While our current results demonstrate that TNF mediates at least a portion of vPD1/IL-12's systemic toxicity, this molecule is also frequently associated with enhanced oncolytic outcomes.[45–49] It is therefore critical to note that we have also recently shown that TNF blockade can actually improve the efficacy of MYXV-based OV.[5] This effect occurs because the high levels of TNF within treated tumors can cause direct necrosis of tumor-infiltrating T cells. Blockade of this TNF therefore improves intratumoral T cell viability and enhances the efficacy of existing anti-tumor T cell responses.[5] Critically, similar results have been shown for other forms of immunotherapy, such as PD-1 based checkpoint blockade.[50–52] TNF blockade therefore has the potential to both reduce toxicities and improve overall therapeutic efficacy of a variety of immunotherapies.

Another of the key findings from our work is that the toxicities induced by vPD1/IL-12 can be alleviated by the clinical available TNF blocker etanercept. These studies were initially conducted because our results indicated that vPD1/IL-12's toxicity required TNFR2. We therefore hypothesized that etanercept, which is a secreted form of TNFR2, would have the highest efficacy at sequestering the specific form of TNF that is mediating these toxicities. It is important to note, however, that there are currently five FDA-approved TNF blockers, which vary in their specificity and applicability.[53] For example, infliximab, adalimumab, and golimumab are all antibodies against TNF, while certolizumab is a similarly designed pegylated antibody fragment. All of these agents are used to treat systemic inflammation and conditions that arise from chronic inflammation; however, their molecular specificities are distinct.[53] For example, etanercept displays a preference for membrane-bound TNF, which is not seen for adalimumab. Additional work is therefore required to further elucidate which FDA-approved TNF-blocking agents might be the best combination with OV. Unfortunately, these experiments are somewhat challenging due to the fact that several of the FDA-approved drugs do not function in murine systems.

In conclusion, in the current work, we present data that have explored phenotypic and molecular toxicities elicited by treatment with a doubly recombinant oncolytic virus, vPD1/IL-12, and how these side effects can be diminished using TNF blockade. This work demonstrates a novel role for TNF in IL-12-mediated toxicities, particularly in the setting of OV. Additionally, in combination with our previous results[5] as well as similar findings in the context of PD1 blockade,[45–49] this work suggests that TNF blockade might be capable of separating the toxicities associated with immunotherapy from its therapeutic efficacy. Additional studies of the optimal methods of applying this finding clinically as well as more comprehensive analyses of the mechanisms involved therefore need to be conducted in the future.

MATERIALS AND METHODS

Cell lines, viral constructs, and reagents

B16/F10 (CRL06475), M3 (CCL-53.1), and YUMM1.7 melanoma cells (CRL-3362) were purchased from the American Type Culture Collection (Manassas, VA, USA). LLC-A9F1 cells (a derivative of parental LLC) were a kind gift from Dr. Mark Rubenstein at the Medical University of South Carolina. MC38B colon cancer cells were obtained from Dr. Aaron Ring at Yale University. BR5 ovarian cancer cells were a kind gift from Dr. Rita Serda at the University of New Mexico Health Sciences Center. All cell lines were cultured in DMEM+10% fetal bovine serum with 1× penicillin-streptomycin-L-glutamine (Mediatech, Manassas, VA, USA). The following depleting antibodies were used: anti-TNF (clone TN3) and anti-IFNγ (clone XMG1.2). They were obtained from Bio X Cell (Lebanon, NH, USA). Etanercept (Enbrel) was obtained from the manufacturer (Amgen, Thousand Oaks, CA, USA). All virus constructs are based on the Lausanne strain of MYXV. Both vGFP and the doubly recombinant vPD1/IL-12 have been described previously.[5,54] Virus was amplified in BSC40 cells and purified using gradient centrifugation as described previously. Viral titer was determined by serial dilution in BSC40 cells. All experiments using virus were conducted under protocols approved by the UNM institutional biosafety committee.

Mouse models

All mice in these studies were between 6 and 10 weeks of age. For all tumor models, 1×10^6 cells from each cell line were injected s.c. into the flanks of syngeneic mice (C57Bl/6 for B16/F10, LLC, and YUMM1.7; DBA for M3; and FVB for BR5). Tumors were allowed to develop, and treatment was initiated when both tumors reached ~25 mm^2, which usually occurred 7–9 days post tumor implantation, with LLC tumors taking around 14–16 days. Treatment consisted of three injections (delivered on days 0, 2, and 4) of 50 μL containing 1×10^7 FFUs of virus injected directly into the larger lesion. Injection of 50 μL of sterile PBS was used as a control. Knockout mice used in these studies include *RAG*$^{-/-}$ (B6.129S7-*Rag1*^{tm1Mom}/J), NSG, *IL-12Rβ1*$^{-/-}$ (B6.129S1-Il12rb1tm1Jm/J), *IFNγ*$^{-/-}$ (B6.129S7-Ifnγ^{tm1Ts}/J), *IFNγR1*$^{-/-}$ (B6.129S7-Ifnγr1^{tm1Agt}/J), *TNF-α*$^{-/-}$ (B6; 129S-*Tnf*^{tm1Gkl}/J), *TNFR1*$^{-/-}$ (C57Bl/6-Tnfrsf1a^{tm1Imx}/J), and *TNFR2*$^{-/-}$ (B6.129S2-Tnfrsf1b^{tm1Mwm}/J). All animal studies were conducted under protocols approved by the UNM institutional animal care and use committee.

Analysis of toxicity

Phenotypic toxicity was determined by analyzing animal body weight and observable body condition. Initial body weight was measured prior to the first viral treatment and subsequently every other day for the duration of the study. Weight is presented as a percent change from the starting weight for each animal. Additional measures of

phenotypic condition were also monitored every other day and included hunched posture, discolored extremities, decreased body temperature, decreased activity, decreased grip strength, poor grooming (ruffled fur), blepharospasm (closed eyes), and changes in stool consistency. Each parameter was scored by severity from 0–5, where 0 meant the symptom was not present, and 5 meant the symptom was severe (Table S1). Scoring was conducted by an investigator blinded to the groups. Scores for all parameters were combined to create an overall "phenotypic toxicity" score. Chemical toxicity was determined by harvesting blood from each animal and analyzing the abundance of various serum chemicals using the Preventative Care Profile Plus Kit (Abaxis, Union City, CA, USA) which measures ALB, ALT, ALP, AST, blood urea nitrogen (BUN), calcium, chloride (Cl^-), creatinine, globulin (GLOB), GLU, potassium (K^+), sodium (Na^+), total carbon dioxide, total bilirubin (TBIL), and TP. Hematological toxicity was determined by harvesting blood from each animal and analyzing the blood content on Abaxis Vetscan HM5, which displays a comprehensive complete blood count including 22 distinct parameters. Chemical and hematological toxicity scores were generated from the data above as follows. Data from four separate toxicity experiments were combined, and the factors that statistically differed between mock and vPD1/IL-12-treated groups were identified using Student's t test ($p < 0.05$). For the chemical toxicity score, these parameters included GLU, ALB, TP, ALT, TBIL, GLOB, BUN, ALP, AST, and Cl^-. For the hematological toxicity score, these parameters included HGB, RBC, HCT, PLT, LYM%, MCH, MCHC, NEU%, PDW, MPV, and PDW%. Subsequently, for each individual experiment, the mean and standard deviation (STD) of each parameter in the mock group was calculated. Each parameter was then assigned a score for each mouse based on the number of standard deviations away from the mock mean (0 < 1 STD, 1 = 1–1.99 STD, 2 > 2 STD). The toxicity score is presented as the sum score of all parameters.

Cytokine and transgene quantification

To quantitate cytokine levels within tumor tissue, excised tumors were mechanically ground over a 40-μm nylon mesh filter, which was then rinsed with 3 mL of PBS. The resulting cell suspension was then centrifuged twice at 3,000 × *g* and the supernatant transferred to a fresh tube. Clarified supernatants were then separated into single-use aliquots for cytokine quantification. IFNγ and IL-12 were quantified using OPTEIA Duo ELISA Kits (BD Biosciences, Franklin Lakes, NJ, USA). Soluble PD1 was quantified using the anti-PD1 DuoSet ELISA (R&D Systems, Minneapolis, MN, USA). TNF cytokine quantification was obtained through the BD Cytometric Bead Array Kit (BD Biosciences). All assays were performed per the manufacturer's recommendations.

Viral quantification

Viral titers were obtained at different time points from excised tumors (injected and contralateral tumor) and tissues (kidney, large and small intestine, lung, heart, liver, and stomach). Each tissue was mechanically ground over a 40-μm mesh, and the resulting cell suspension was then centrifuged at 3 000 × *g*. The supernatant was removed, and the resulting cell pellet was lysed through three rounds of sequential freezing-thawing and sonication. Infectious virus in each sample was then quantified through serial dilution and titer assays on BSC40 cells. Viral titers are presented as total FFUs recovered from each sample.

Bone marrow transplantation

For irradiation, mice received 8.5 Gy split into two doses of 4.25 Gy, 3 h apart. 24 h post irradiation, recipient mice were transplanted with 3×10^6 bone marrow cells extracted from the femora of donor mice. Recipient mice were placed on Baytril for 2 weeks post transplantation to prevent infection. Chimerism was confirmed 6 weeks post transplantation by assaying Thy1.1 and Thy1.2 ratios from whole blood. Mice were then implanted contralaterally with B16/F10 mouse melanoma cells and treated as above.

DATA AND CODE AVAILABILITY

All data and reagents required to interpret, verify, and extend the research in the current article are freely available to readers.

ACKNOWLEDGMENTS

This work was funded by grants to E.B., including AI142387, CA268163, CA276134, and CA194090 from the NIH as well as RSG-17-047-01-MPC from the American Cancer Society. The work was also supported by a UNM comprehensive cancer center support grant (P30-CA118100).

AUTHOR CONTRIBUTIONS

M.V.C., investigation, data curation, formal analysis, methodology, and writing; C.F., investigation and methodology; M.Y.B., methodology and resources; E.B., conceptualization, project administration, funding acquisition, and supervision.

DECLARATION OF INTERESTS

E.B. holds intellectual property rights to the recombinant oncolytic myxoma virus encoding soluble PD1 and IL-12. E.B. also holds intellectual property rights to a variety of other recombinant oncolytic myxoma viruses that are not relevant to the current manuscript.

SUPPLEMENTAL INFORMATION

Supplemental information can be found online at https://doi.org/10.1016/j.omton.2024.200866.

REFERENCES

1. Liu, T.C., Galanis, E., and Kirn, D. (2007). Clinical trial results with oncolytic virotherapy: a century of promise, a decade of progress. Nat. Clin. Pract. Oncol. *4*, 101–117. https://doi.org/10.1038/ncponc0736.

2. Melcher, A., Parato, K., Rooney, C.M., and Bell, J.C. (2011). Thunder and lightning: immunotherapy and oncolytic viruses collide. Mol. Ther. *19*, 1008–1016. https://doi.org/10.1038/mt.2011.65.

3. Diallo, J.S., Le Boeuf, F., Lai, F., Cox, J., Vaha-Koskela, M., Abdelbary, H., MacTavish, H., Waite, K., Falls, T., Wang, J., et al. (2010). A high-throughput pharmacoviral approach identifies novel oncolytic virus sensitizers. Mol. Ther. *18*, 1123–1129. https://doi.org/10.1038/mt.2010.67.

4. Pandha, H.S., Heinemann, L., Simpson, G.R., Melcher, A., Prestwich, R., Errington, F., Coffey, M., Harrington, K.J., and Morgan, R. (2009). Synergistic effects of oncolytic reovirus and cisplatin chemotherapy in murine malignant melanoma. Clin. Cancer Res. *15*, 6158–6166. https://doi.org/10.1158/1078-0432.CCR-09-0796.

5. Valenzuela-Cardenas, M., Gowan, C., Dryja, P., Bartee, M.Y., and Bartee, E. (2022). TNF blockade enhances the efficacy of myxoma virus-based oncolytic virotherapy. J. Immunother. Cancer *10*, e004770. https://doi.org/10.1136/jitc-2022-004770.

6. Wang, D.Y., Johnson, D.B., and Davis, E.J. (2018). Toxicities Associated With PD-1/PD-L1 Blockade. Cancer J. *24*, 36–40. https://doi.org/10.1097/PPO.0000000000000296.

7. Naidoo, J., Page, D.B., Li, B.T., Connell, L.C., Schindler, K., Lacouture, M.E., Postow, M.A., and Wolchok, J.D. (2015). Toxicities of the anti-PD-1 and anti-PD-L1 immune checkpoint antibodies. Ann. Oncol. *26*, 2375–2391. https://doi.org/10.1093/annonc/mdv383.

8. Yin, Q., Wu, L., Han, L., Zheng, X., Tong, R., Li, L., Bai, L., and Bian, Y. (2023). Immune-related adverse events of immune checkpoint inhibitors: a review. Front. Immunol. *14*, 1167975. https://doi.org/10.3389/fimmu.2023.1167975.

9. Jia, Z., Ragoonanan, D., Mahadeo, K.M., Gill, J., Gorlick, R., Shpal, E., and Li, S. (2022). IL12 immune therapy clinical trial review: Novel strategies for avoiding CRS-associated cytokines. Front. Immunol. *13*, 952231. https://doi.org/10.3389/fimmu.2022.952231.

10. Lenzi, R., Edwards, R., June, C., Seiden, M.V., Garcia, M.E., Rosenblum, M., and Freedman, R.S. (2007). Phase II study of intraperitoneal recombinant interleukin-12 (rhIL-12) in patients with peritoneal carcinomatosis (residual disease < 1 cm) associated with ovarian cancer or primary peritoneal carcinoma. J. Transl. Med. *5*, 66. https://doi.org/10.1186/1479-5876-5-66.

11. Lasek, W., Zagożdżon, R., and Jakobisiak, M. (2014). Interleukin 12: still a promising candidate for tumor immunotherapy? Cancer Immunol. Immunother. *63*, 419–435. https://doi.org/10.1007/s00262-014-1523-1.

12. Robertson, M.J., Pelloso, D., Abonour, R., Hromas, R.A., Nelson, R.P., Jr., Wood, L., and Cornetta, K. (2002). Interleukin 12 immunotherapy after autologous stem cell transplantation for hematological malignancies. Clin. Cancer Res. *8*, 3383–3393.

13. Van Herpen, C.M., Huijbens, R., Looman, M., De Vries, J., Marres, H., Van De Ven, J., Hermsen, R., Adema, G.J., and De Mulder, P.H. (2003). Pharmacokinetics and immunological aspects of a phase Ib study with intratumoral administration of recombinant human interleukin-12 in patients with head and neck squamous cell carcinoma: a decrease of T-bet in peripheral blood mononuclear cells. Clin. Cancer Res. *9*, 2950–2956.

14. Atkins, M.B., Robertson, M.J., Gordon, M., Lotze, M.T., DeCoste, M., DuBois, J.S., Ritz, J., Sandler, A.B., Edington, H.D., Garzone, P.D., et al. (1997). Phase I evaluation of intravenous recombinant human interleukin 12 in patients with advanced malignancies. Clin. Cancer Res. *3*, 409–417.

15. Haicheur, N., Escudier, B., Dorval, T., Negrier, S., De Mulder, P.H., Dupuy, J.M., Novick, D., Guillot, T., Wolf, S., Pouillart, P., et al. (2000). Cytokines and soluble cytokine receptor induction after IL-12 administration in cancer patients. Clin. Exp. Immunol. *119*, 28–37. https://doi.org/10.1046/j.1365-2249.2000.01112.x.

16. Parihar, R., Nadella, P., Lewis, A., Jensen, R., De Hoff, C., Dierksheide, J.E., VanBuskirk, A.M., Magro, C.M., Young, D.C., Shapiro, C.L., and Carson, W.E., 3rd (2004). A phase I study of interleukin 12 with trastuzumab in patients with human epidermal growth factor receptor-2-overexpressing malignancies: analysis of sustained interferon gamma production in a subset of patients. Clin. Cancer Res. *10*, 5027–5037. https://doi.org/10.1158/1078-0432.CCR-04-0265.

17. Rahman, M.M., and McFadden, G. (2020). Oncolytic Virotherapy with Myxoma Virus. J. Clin. Med. *9*, 171. https://doi.org/10.3390/jcm9010171.

18. Lawler, S.E., Speranza, M.C., Cho, C.F., and Chiocca, E.A. (2017). Oncolytic Viruses in Cancer Treatment: A Review. JAMA Oncol. *3*, 841–849. https://doi.org/10.1001/jamaoncol.2016.2064.

19. Bommareddy, P.K., Shettigar, M., and Kaufman, H.L. (2018). Integrating oncolytic viruses in combination cancer immunotherapy. Nat. Rev. Immunol. *18*, 498–513. https://doi.org/10.1038/s41577-018-0014-6.

20. Martin, N.T., and Bell, J.C. (2018). Oncolytic Virus Combination Therapy: Killing One Bird with Two Stones. Mol. Ther. *26*, 1414–1422. https://doi.org/10.1016/j.ymthe.2018.04.001.

21. MacEwan, D.J. (2002). TNF ligands and receptors–a matter of life and death. Br. J. Pharmacol. *135*, 855–875. https://doi.org/10.1038/sj.bjp.0704549.

22. Gough, P., and Myles, I.A. (2020). Tumor Necrosis Factor Receptors: Pleiotropic Signaling Complexes and Their Differential Effects. Front. Immunol. *11*, 585880. https://doi.org/10.3389/fimmu.2020.585880.

23. Brasseit, J., Althaus-Steiner, E., Faderl, M., Dickgreber, N., Saurer, L., Genitsch, V., Dolowschiak, T., Li, H., Finke, D., Hardt, W.D., et al. (2016). CD4 T cells are required for both development and maintenance of disease in a new mouse model of reversible colitis. Mucosal Immunol. *9*, 689–701. https://doi.org/10.1038/mi.2015.93.

24. Jenks, S. (1996). After initial setback, IL-12 regaining popularity. J. Natl. Cancer Inst. *88*, 576–577. https://doi.org/10.1093/jnci/88.9.576.

25. Rodriguez-Galan, M.C., Reynolds, D., Correa, S.G., Iribarren, P., Watanabe, M., and Young, H.A. (2009). Coexpression of IL-18 strongly attenuates IL-12-induced systemic toxicity through a rapid induction of IL-10 without affecting its antitumor capacity. J. Immunol. *183*, 740–748. https://doi.org/10.4049/jimmunol.0804166.

26. Gollob, J.A., Veenstra, K.G., Parker, R.A., Mier, J.W., McDermott, D.F., Clancy, D., Tutin, L., Koon, H., and Atkins, M.B. (2003). Phase I trial of concurrent twice-weekly recombinant human interleukin-12 plus low-dose IL-2 in patients with melanoma or renal cell carcinoma. J. Clin. Oncol. *21*, 2564–2573. https://doi.org/10.1200/JCO.2003.12.119.

27. Motzer, R.J., Rakhit, A., Schwartz, L.H., Olencki, T., Malone, T.M., Sandstrom, K., Nadeau, R., Parmar, H., and Bukowski, R. (1998). Phase I trial of subcutaneous recombinant human interleukin-12 in patients with advanced renal cell carcinoma. Clin. Cancer Res. *4*, 1183–1191.

28. Portielje, J.E.A., Lamers, C.H.J., Kruit, W.H.J., Sparreboom, A., Bolhuis, R.L.H., Stoter, G., Huber, C., and Gratama, J.W. (2003). Repeated administrations of interleukin (IL)-12 are associated with persistently elevated plasma levels of IL-10 and declining IFN-gamma, tumor necrosis factor-alpha, IL-6, and IL-8 responses. Clin. Cancer Res. *9*, 76–83.

29. Bramson, J., Hitt, M., Gallichan, W.S., Rosenthal, K.L., Gauldie, J., and Graham, F.L. (1996). Construction of a double recombinant adenovirus vector expressing a heterodimeric cytokine: in vitro and in vivo production of biologically active interleukin-12. Hum. Gene Ther. *7*, 333–342. https://doi.org/10.1089/hum.1996.7.3-333.

30. Osada, T., Berglund, P., Morse, M.A., Hubby, B., Lewis, W., Niedzwiecki, D., Yang, X.Y., Hobeika, A., Burnett, B., Devi, G.R., et al. (2012). Co-delivery of antigen and IL-12 by Venezuelan equine encephalitis virus replicon particles enhances antigen-specific immune responses and antitumor effects. Cancer Immunol. Immunother. *61*, 1941–1951. https://doi.org/10.1007/s00262-012-1248-y.

31. Lyerly, H.K., Osada, T., and Hartman, Z.C. (2019). Right Time and Place for IL12: Targeted Delivery Stimulates Immune Therapy. Clin. Cancer Res. *25*, 9–11. https://doi.org/10.1158/1078-0432.CCR-18-2819.

32. Lai, I., Swaminathan, S., Baylot, V., Mosley, A., Dhanasekaran, R., Gabay, M., and Felsher, D.W. (2018). Lipid nanoparticles that deliver IL-12 messenger RNA suppress tumorigenesis in MYC oncogene-driven hepatocellular carcinoma. J. Immunother. Cancer *6*, 125. https://doi.org/10.1186/s40425-018-0431-x.

33. Caruso, M., Pham-Nguyen, K., Kwong, Y.L., Xu, B., Kosai, K.I., Finegold, M., Woo, S.L., and Chen, S.H. (1996). Adenovirus-mediated interleukin-12 gene therapy for metastatic colon carcinoma. Proc. Natl. Acad. Sci. USA *93*, 11302–11306. https://doi.org/10.1073/pnas.93.21.11302.

34. Jarnagin, W.R., Zager, J.S., Klimstra, D., Delman, K.A., Malhotra, S., Ebright, M., Little, S., DeRubertis, B., Stanziale, S.F., Hezel, M., et al. (2003). Neoadjuvant treatment of hepatic malignancy: an oncolytic herpes simplex virus expressing IL-12 effectively treats the parent tumor and protects against recurrence-after resection. Cancer Gene Ther. *10*, 215–223. https://doi.org/10.1038/sj.cgt.7700558.

35. Chen, B., Timiryasova, T.M., Gridley, D.S., Andres, M.L., Dutta-Roy, R., and Fodor, I. (2001). Evaluation of cytokine toxicity induced by vaccinia virus-mediated IL-2 and IL-12 antitumour immunotherapy. Cytokine *15*, 305–314. https://doi.org/10.1006/cyto.2001.0906.

36. Chen, B., Timiryasova, T.M., Haghighat, P., Andres, M.L., Kajioka, E.H., Dutta-Roy, R., Gridley, D.S., and Fodor, I. (2001). Low-dose vaccinia virus-mediated cytokine gene therapy of glioma. J. Immunother. *24*, 46–57. https://doi.org/10.1097/00002371-200101000-00006.

37. Waehler, R., Ittrich, H., Mueller, L., Krupski, G., Ameis, D., and Schnieders, F. (2005). Low-dose adenoviral immunotherapy of rat hepatocellular carcinoma using single-chain interleukin-12. Hum. Gene Ther. *16*, 307–317. https://doi.org/10.1089/hum.2005.16.307.

38. Cheng, T.L., and Roffler, S. (2008). Membrane-tethered proteins for basic research, imaging, and therapy. Med. Res. Rev. *28*, 885–928. https://doi.org/10.1002/med.20127.

39. Wang, P., Li, X., Wang, J., Gao, D., Li, Y., Li, H., Chu, Y., Zhang, Z., Liu, H., Jiang, G., et al. (2017). Re-designing Interleukin-12 to enhance its safety and potential as an anti-tumor immunotherapeutic agent. Nat. Commun. *8*, 1395. https://doi.org/10.1038/s41467-017-01385-8.

40. Car, B.D., Eng, V.M., Schnyder, B., LeHir, M., Shakhov, A.N., Woerly, G., Huang, S., Aguet, M., Anderson, T.D., and Ryffel, B. (1995). Role of interferon-gamma in interleukin 12-induced pathology in mice. Am. J. Pathol. *147*, 1693–1707.

41. Car, B.D., Eng, V.M., Schnyder, B., Ozmen, L., Huang, S., Gallay, P., Heumann, D., Aguet, M., and Ryffel, B. (1994). Interferon gamma receptor deficient mice are resistant to endotoxic shock. J. Exp. Med. *179*, 1437–1444. https://doi.org/10.1084/jem.179.5.1437.

42. Ryffel, B. (1997). Interleukin-12: role of interferon-gamma in IL-12 adverse effects. Clin. Immunol. Immunopathol. *83*, 18–20. https://doi.org/10.1006/clin.1996.4306.

43. Hailemichael, Y., Johnson, D.H., Abdel-Wahab, N., Foo, W.C., Bentebibel, S.E., Daher, M., Haymaker, C., Wani, K., Saberian, C., Ogata, D., et al. (2022). Interleukin-6 blockade abrogates immunotherapy toxicity and promotes tumor immunity. Cancer Cell *40*, 509–523.e6. https://doi.org/10.1016/j.ccell.2022.04.004.

44. Orange, J.S., Salazar-Mather, T.P., Opal, S.M., Spencer, R.L., Miller, A.H., McEwen, B.S., and Biron, C.A. (1995). Mechanism of interleukin 12-mediated toxicities during experimental viral infections: role of tumor necrosis factor and glucocorticoids. J. Exp. Med. *181*, 901–914. https://doi.org/10.1084/jem.181.3.901.

45. Beug, S.T., Pichette, S.J., St-Jean, M., Holbrook, J., Walker, D.E., LaCasse, E.C., and Korneluk, R.G. (2018). Combination of IAP Antagonists and TNF-alpha-Armed Oncolytic Viruses Induce Tumor Vascular Shutdown and Tumor Regression. Mol. Ther. Oncolytics *10*, 28–39. https://doi.org/10.1016/j.omto.2018.06.002.

46. Christie, J.D., Appel, N., Canter, H., Achi, J.G., Elliott, N.M., de Matos, A.L., Franco, L., Kilbourne, J., Lowe, K., Rahman, M.M., et al. (2021). Systemic delivery of TNF-armed myxoma virus plus immune checkpoint inhibitor eliminates lung metastatic mouse osteosarcoma. Mol. Ther. Oncolytics *22*, 539–554. https://doi.org/10.1016/j.omto.2021.07.014.

47. Han, Z.Q., Assenberg, M., Liu, B.L., Wang, Y.B., Simpson, G., Thomas, S., and Coffin, R.S. (2007). Development of a second-generation oncolytic Herpes simplex virus expressing TNFalpha for cancer therapy. J. Gene Med. *9*, 99–106. https://doi.org/10.1002/jgm.999.

48. Havunen, R., Siurala, M., Sorsa, S., Grönberg-Vähä-Koskela, S., Behr, M., Tähtinen, S., Santos, J.M., Karell, P., Rusanen, J., Nettelbeck, D.M., et al. (2017). Oncolytic Adenoviruses Armed with Tumor Necrosis Factor Alpha and Interleukin-2 Enable Successful Adoptive Cell Therapy. Mol. Ther. Oncolytics *4*, 77–86. https://doi.org/10.1016/j.omto.2016.12.004.

49. Li, S., Qi, Z., Li, H., Hu, J., Wang, D., Wang, X., and Feng, Z. (2015). Conditionally replicating oncolytic adenoviral vector expressing arresten and tumor necrosis factor-related apoptosis-inducing ligand experimentally suppresses lung carcinoma progression. Mol. Med. Rep. *12*, 2068–2074. https://doi.org/10.3892/mmr.2015.3624.

50. Perez-Ruiz, E., Minute, L., Otano, I., Alvarez, M., Ochoa, M.C., Belsue, V., de Andrea, C., Rodriguez-Ruiz, M.E., Perez-Gracia, J.L., Marquez-Rodas, I., et al. (2019). Prophylactic TNF blockade uncouples efficacy and toxicity in dual CTLA-4 and PD-1 immunotherapy. Nature *569*, 428–432. https://doi.org/10.1038/s41586-019-1162-y.

51. Alvarez, M., Otano, I., Minute, L., Ochoa, M.C., Perez-Ruiz, E., Melero, I., and Berraondo, P. (2019). Impact of prophylactic TNF blockade in the dual PD-1 and CTLA-4 immunotherapy efficacy and toxicity. Cell Stress *3*, 236–239. https://doi.org/10.15698/cst2019.07.193.

52. Bertrand, F., Montfort, A., Marcheteau, E., Imbert, C., Gilhodes, J., Filleron, T., Rochaix, P., Andrieu-Abadie, N., Levade, T., Meyer, N., et al. (2017). TNFalpha blockade overcomes resistance to anti-PD-1 in experimental melanoma. Nat. Commun. *8*, 2256. https://doi.org/10.1038/s41467-017-02358-7.

53. Gerriets, V., Goyal, A., and Khaddour, K. (2024). Tumor Necrosis Factor Inhibitors. In StatPearls (Treasure Island). Ineligible Companies. Disclosure: Amandeep Goyal Declares No Relevant Financial Relationships with Ineligible Companies. Disclosure: Karam Khaddour Declares No Relevant Financial Relationships with Ineligible Companies.

54. Bartee, M.Y., Dunlap, K.M., and Bartee, E. (2017). Tumor-Localized Secretion of Soluble PD1 Enhances Oncolytic Virotherapy. Cancer Res. *77*, 2952–2963. https://doi.org/10.1158/0008-5472.CAN-16-1638.